Title

ROTATIONAL RELAXATION IN SUPERSONIC BEAMS OF HYDROGEN BY HIGH RESOLUTION PHOTOELECTRON SPECTROSCOPY

Author

Pollard, J.E.

Publication Date

1982-06-01

Lawrence Berkeley Laboratory
UNIVERSITY OF CALIFORNIA

Materials & Molecular Research Division

Submitted to the Journal of Chemical Physics

ROTATIONAL RELAXATION IN SUPERSONIC BEAMS OF HYDROGEN BY HIGH RESOLUTION PHOTOELECTRON SPECTROSCOPY

J.E. Pollard, D.J. Trevor, Y.T. Lee,
and D.A. Shirley

June 1982

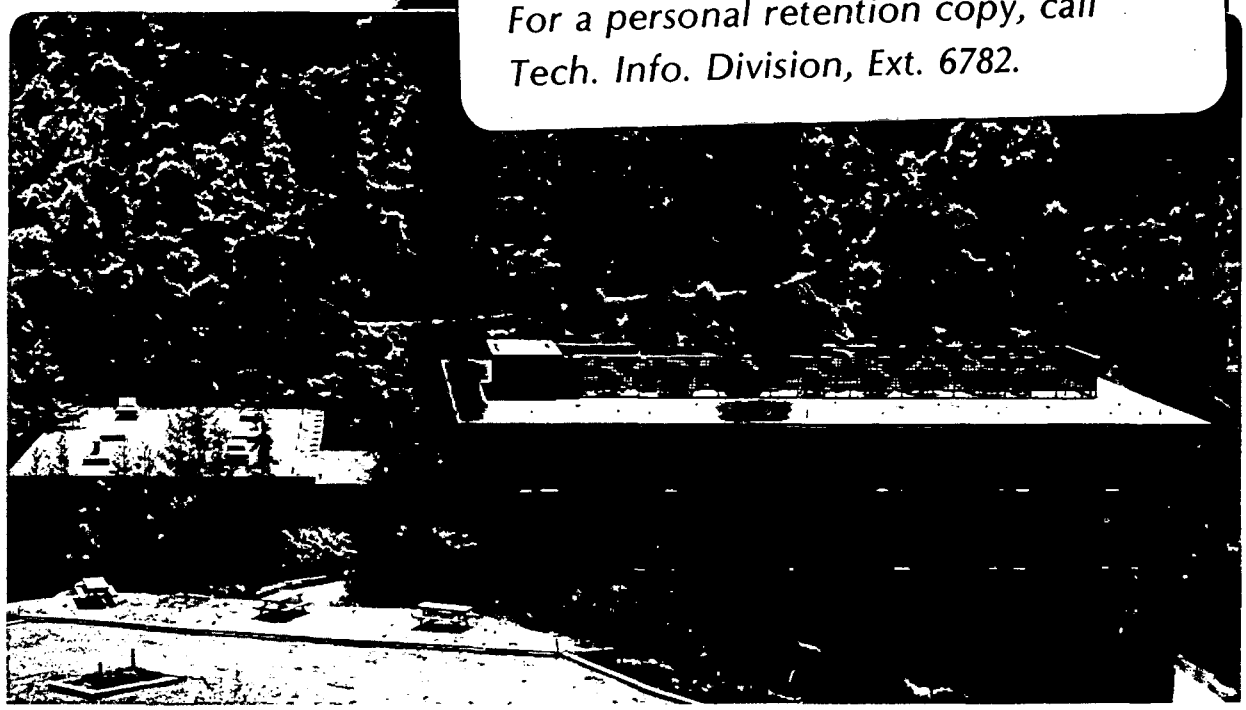

Prepared for the U.S. Department of Energy under Contract DE-AC03-76SF00098

DISCLAIMER

LBL-14279

ROTATIONAL RELAXATION IN SUPERSONIC BEAMS OF HYDROGEN BY HIGH RESOLUTION PHOTOELECTRON SPECTROSCOPY

J. E. Pollard, D. J. Trevor,
Y. T. Lee, and D. A. Shirley

Materials and Molecular Research Division
Lawrence Berkeley Laboratory
and
Department of Chemistry
University of California
Berkeley, California 94720

June 1982

This work is supported by the Director, Office of Energy Research, Office of Basic Energy Sciences, Chemical Sciences Division of the U.S. Department of Energy under Contract No. DE-AC03-76SF00098.

ROTATIONAL RELAXATION IN SUPERSONIC BEAMS OF HYDROGEN BY HIGH RESOLUTION PHOTOELECTRON SPECTROSCOPY

J. E. Pollard, D. J. Trevor,
Y. T. Lee, and D. A. Shirley

Materials and Molecular Research Division
Lawrence Berkeley Laboratory
and
Department of Chemistry
University of California
Berkeley, California 94720

ABSTRACT

The rotational relaxation of n-H_2, p-H_2, HD, and n-D_2 in a free jet expansion was studied by means of rotationally-resolved photoelectron spectroscopy using a collimated supersonic molecular beam. Rotational state distributions were determined from the relative intensities of the Q branch rotational components for a wide range of stagnation pressures with nozzle temperatures from 300K to 700K. Significant deviations from a Boltzmann distribution were observed for those cases in which the degree of rotational relaxation was substantial. HD was found to relax after undergoing only one-tenth of the number of collisions required to relax H_2 or D_2. The relaxation of p-H_2 was modeled using the state-to-state rate constants method of Rabitz and Lam, which was confirmed to be quite effective in accounting for the experimentally observed population distributions.

I. INTRODUCTION

A free jet expansion constitutes a system in which the internal degrees of freedom of the molecules are initially in contact with a rapidly cooling translational bath. In the early (collisional) part of the expansion the internal modes can relax by transferring energy into translation until the collisions become very infrequent, and communication with the bath is lost. The details of this relaxation process can be elucidated by measuring the rotational and vibrational state distributions of the molecules in the beam as functions of the stagnation conditions. Such experiments have been performed for a number of molecular systems using a variety of spectroscopic techniques.[1] We have recently succeeded in obtaining rotationally-resolved photoelectron spectra from supersonic beams of hydrogen,[2] and the present investigation is an extension of this technique to the study of rotational relaxation in supersonic expansions of this simple and important molecule.

Hydrogen is in several respects an unusual system. The very large rotational energy spacings allow only a few levels to be thermally populated at room temperature. Vibrational excitation is negligible for H_2 below 1000K. The large rotational energy gaps and the small anisotropy of the interaction potential make the R-T energy transfer inefficient compared to heavier molecules. In addition the isotopic species of molecular hydrogen should exhibit substantially different relaxation behaviors because of the variations in the spacings of the rotational energy levels and in the anisotropy of the potential.

Finally, for H_2 and D_2 the lack of conversion between the ortho and para forms will lead to large deviations from a Boltzmann distribution of rotational states for high Mach number expansions.

There have been several previous experimental investigations of rotational relaxation in beams of hydrogen. Gallagher and Fenn[3] measured time-of-flight velocity distributions for n-H_2 at stagnation temperatures from 300K to 1900K and used the energy balance criterion to derive rotational temperatures and collision numbers. They found that the rotational collision number increases from 300 to 500 over this temperature range. Buck et al.[4] performed time-of-flight measurements on HD, n-D_2, and o-D_2 with stagnation temperatures of 300K or below and, like Gallagher and Fenn, assumed a Boltzmann rotational distribution to derive the state populations for D_2. Verberne, et al.[5] used molecular beam magnetic resonance to measure the populations of n-H_2 with stagnation temperatures from 300K to 1000K and found that the distribution could not be characterized by a unique rotational temperature. Godfried, et al.[6] used Raman scattering to measure the number density and populations in free jets of n-H_2 and n-D_2 with a stagnation temperature of 293K. They compared their results with the predictions of a model which treats the time evolution of the state populations and uses a single rotational collision number. They also reported an axial density profile for n-H_2 which corresponds to that expected for a monatomic ($C_p/C_v = 1.67$) expansion. Huber-Wälchli and Nibeler[7] measured CARS spectra of n-H_2 and n-D_2 in free jets with a 300K stagnation temperature. They analyzed their data in terms of

the rotational temperature which served as an input parameter in their CARS spectral simulation.

The minimum number density required for Raman or CARS experiments on hydrogen is approximately 10^{16} cm^{-3}, so that it is necessary to use an unskimmed free jet. The present measurements employ a collimated molecular beam which more closely approximates the experimental arrangement common to crossed beam scattering studies. The number density ranges from about 10^{11} to 10^{13} cm^{-3}. We report level populations for fully expanded jets of n-H_2 and n-D_2 over a wider range of stagnation conditions than have been reported previously, and we also extend the population measurements to p-H_2 and HD for the first time. We observe departures from a Boltzmann distribution for strong expansions. The results for p-H_2 are analyzed in terms of the theoretical framework of Rabitz and Lam,[8] which uses a set of state-to-state rate constants and combines the master kinetic equations with the equations of fluid mechanics.

Experimental parameters are described in Section II, and results are given and discussed in Section III. The rotational relaxation of p-H_2 is modeled in Section IV, using the theory of Rabitz and Lam.

II. EXPERIMENTAL

The photoelectron spectrometer used in this work was described in detail in an earlier publication.[9] The electron energy analyzer was a double electrostatic deflector with multichannel detection and was operated at a resolution of 11 meV FWHM (for Ar) with HeIα (584Å, 21.217 eV) light. Photoelectrons were sampled at an angle of 90° with respect to the photon beam. Two beam source configurations were used: (1) a 70-μm-diam nozzle located 6.4 mm from the tip of a 0.66-mm-diam X 6.4-mm-tall conical skimmer, and (2) a 40-μm-diam nozzle located 9.6 mm from the tip of a 0.66-mm-diam X 12.7-mm-tall conical skimmer. The photon beam crossed the molecular beam at 32 mm downstream from the nozzle in configuration (1) and at 41 mm downstream from the nozzle in configuration (2). The nozzles were made from molybdenum electron microscope apertures (Ted Pella Inc.), and were of the converging type. The pressure in the beam source exhaust chamber was typically less than 5×10^{-4} torr, and in the main chamber the pressure was less than 2×10^{-5} torr. The nozzle could be heated to a maximum of 700K with a coil of non-inductively-wound two-wire Semflex heater cable (Semco Inc.). Some care was necessary when running at high temperature, because the electron kinetic energy offset drifted rapidly as surfaces near the ionization region warmed up. For this reason the scan time was usually restricted to 30 minutes or less when running with the heated nozzle. The samples and other experimental details were the same as we used in our previous work on hydrogen.[2] High temperature scans were not feasible for HD because the

sample converted to a mixture of HD, H_2, and D_2 when the nozzle was heated. Similarly, we did not attempt to run p-H_2 above room temperature, because the conversion to n-H_2 was expected to be rapid. The evident dissociation of hydrogen behind the high temperature nozzle should not affect the ortho-para ratio in the rotationally-relaxed n-H_2 and n-D_2 beams, because the relaxation is confined primarily to the region downstream of the nozzle throat where the molecules are no longer colliding with the heated metal surfaces.

III. RESULTS AND DISCUSSION

Rotational populations were determined from the relative intensities of the Q branch ($\Delta J=0$) components for a selected vibrational state of the molecular ion. The Q branch can be more fully resolved for the higher v-states, until the point at which the adjacent vibrational transitions begin to overlap. The optimal v-states for this experiment were $H_2^+(v'=5)$, $HD^+(v'=7)$, and $D_2^+(v'=8)$. The areas of the rotational components were calculated by least-squares fitting of the spectra using an empirically derived lineshape function which we have described previously.[2] Standard deviations of the peak intensities from the least-squares fits were generally in the range of 1-3% of the area of a given rotational component, although for those cases where the population of the state was less than 1%, the standard deviation was about 10-20% of the area. The S branch ($\Delta J=+2$) was also included in the fit. It contributed about 4% of the total area for H_2 and about 2% for HD and D_2. To convert the photoelectron intensities measured at the present 90° angular geometry to rotational populations it is necessary to consider the rotational dependence of the cross section, σ_J, and the photoelectron asymmetry parameter, β_J. The observed intensity of a given Q branch transition is proportional to the product of the rotational level population and the factor $\sigma_J(1 + \beta_J/4)$. Itikawa[10] has given theoretical values of σ_J and β_J at $\lambda=584$Å for $H_2^+(v'=5)$ which indicate that the corrections necessary for obtaining the rotational population from the photoelectron intensities measured at 90° are less than 1-2% of the intensity of each rotational

component. An approximate experimental verification of Itikawa's cross sections has been reported by Morioka, et al.[11] In order to judge whether a correction was warranted for the present data, we compared our measured intensities at 297K and 25 torr stagnation conditions (70 μm nozzle) with the populations derived from a Boltzmann distribution, assuming a 3:1 ortho-para ratio for n-H_2 and 2:1 ortho-para ratio for n-D_2. For n-H_2, p-H_2, and n-D_2 the results agreed with a Boltzmann distribution to within the statistical uncertainty of the data, although for HD a systematic deviation was noted because the rotational distribution had relaxed to some extent even at 25 torr backing pressure. Thus we applied no correction for the rotational dependence of σ_J and β_J and used the Q branch intensities directly to determine the populations.

Fig. 1 shows a series of spectra which are typical of the data obtained in this experiment. The $H_2^+(v'=5)$ transition from n-H_2 at 696K is shown for several stagnation pressures for which the rotational relaxation is particularly dramatic.

Table I lists the rotational energies and degeneracies which were used in the analysis of the rotational population data.

A. n-H_2 and n-D_2

The rotational populations measured for n-H_2 and n-D_2 expanded from 297K through the 70 μm nozzle are shown in Fig. 2 as functions of pd, the product of the stagnation pressure (p) and the nozzle diameter (d). At the lowest observed pd there is only a slight relaxation of

the rotational energy, and the populations are very close to those expected for a Boltzmann distribution at 297K. As pd is increased the levels relax, but the populations cannot generally be described by a unique Boltzmann temperature. This is demonstrated in Fig. 3, which shows the measured $\ln(n_J/g_J)$ vs. E_J at two nozzle temperatures for n-H_2 and n-D_2. These plots would be linear if there were a unique rotational temperature, but in fact a positive curvature is observed in each case. The R-T energy transfer is therefore less efficient for the higher rotational levels, which is in accord with the fact that the energy gaps are higher for these states. Another way of visualizing the non-Boltzmann nature of the population distributions is to use the two-level temperature relative to the J=0 level, T_{J0}, which is defined by

$$n_J/n_0 = (g_J/g_0) \exp(-E_J/kT_{J0}) \qquad (1)$$

T_{J0} is shown in Fig. 4 for the same data sets that were presented as Boltzmann-type plots in Fig. 3, and it is apparent that T_{J0} increases appreciably with increasing J.

The average rotational energy is given by $E = \sum_J n_J E_J$. We wish to correlate this quantity with a parameter that includes the effects of the three variables investigated in this work -- the stagnation pressure, temperature, and nozzle diameter. The inverse Knudsen number, $(Kn_0)^{-1}$, is an appropriate scaling parameter for this purpose. $(Kn_0)^{-1}$

is the ratio of the nozzle diameter, d, to the mean free path, Λ_0. It is given by

$$(Kn_0)^{-1} = d/\Lambda_0 = \sqrt{2}\ \pi\ a^2\ p\ d\ /\ k\ T$$
$$= 36800 \times p(torr) \times d(cm)\ /\ T(K) \qquad (2)$$

where a = 2.93Å is the gas kinetic collision diameter (from Gallagher and Fenn[3]). $(Kn_0)^{-1}$ is very roughly the number of collisions that a molecule undergoes in the expansion. Figs. 5 and 6 show the results of plotting the fraction of retained rotational energy, $(E - E_0)/(E_T - E_0)$, against the inverse Knudsen number for n-H_2 and n-D_2. E_T and E_0 are the rotational energy at the stagnation temperature and at zero K, respectively (assuming no ortho-para conversion). These plots are seen to be fairly successful in correlating the final rotational energy with the stagnation conditions, although some systematic deviations are noted. With the exception of the results for n-H_2 at 297K the data points corresponding to the 70 μm nozzle have higher rotational energies than those for the 40 μm nozzle at the same $(Kn_0)^{-1}$. A likely source of this difference is the skimmer interference, which we expect to be less important for the configuration used with the 40 μm nozzle (described in Section II). Using $(Kn_0)^{-1}$ as the scaling parameter does not take into account the variation of the rotational collision number with temperature. The data for n-H_2 in the high $(Kn_0)^{-1}$ region are consistent with the observation of Gallagher and Fenn[3] that the rotational collision number increases slightly over our temperature range.

The data for n-D_2 do not exemplify this trend however. A difficulty which applies only to D_2 is that the rotational levels above J=6 are not observed, because they overlap with the next vibrational state. Although these levels contribute only about 4% of the total intensity even at 694K, the fraction of the rotational energy residing in these states is about 0.5% at 297K, 5% at 475K, and 15% at 694K.

Before leaving n-H_2 and n-D_2 we list in Table II some examples of rotational population distributions for high Mach number expansions. In general we observed that the intensity of the beam was reduced and the rotational energy of the beam was increased for pressures higher than those listed, due to collisions with the background gas molecules in the region between the nozzle and the skimmer. It will be noted that the ortho-para ratios exhibit some variation around the expected values of 3:1 for H_2 and 2:1 for D_2. This is attributed to error arising from the deconvolution of the J=0 and J=1 transitions which are not resolved in the spectra. We generally obtained the correct ortho-para ratio for the less fully relaxed cases where the intensity is spread out over several well-resolved transitions.

B. HD

The rotational populations of HD as a function of pd are shown in Fig. 7 for the case of the 70 μm nozzle at 297K. The populations measured at the lowest pd in Fig. 7 have relaxed somewhat from the initial thermal distribution, even though H_2 and D_2 do not show any relaxation under these conditions. The departure from a Boltzmann distribution

is also more pronounced for HD, as is seen in Fig. 8 which shows $\ln(n_J/g_J)$ vs. E_J at several stagnation pressures. We again observe positive curvature in these plots, showing that the relaxation is least effective for the highest rotational levels. Fig. 9 shows the rotational energy as a function of $(Kn_0)^{-1}$, comparing the results for HD and p-H_2. These molecules are alike in the sense that both would have a rotational energy of zero at zero K, so that there are no complications from an "ortho-para" effect. The major difference between them is that the rotational constant is effectively four times larger for p-H_2 than for HD. The result of this difference in energy gaps is reflected in Fig. 9, which shows that to remove half of the rotational energy ten times as many collisions are needed for p-H_2 as for HD. The relaxation of HD is also facilitated by the fact that it rotates about a center of mass which is displaced from the geometrical center of the molecule. This additional anisotropy in the interaction potential for HD leads to a larger rotational relaxation cross section than is found for the homonuclear species.

IV. MODELING THE RELAXATION OF p-H_2

Rabitz and Lam[8] have given a theoretical method for simulating the rotational relaxation of hydrogen in a free jet expansion, which we have applied to p-H_2 to gain a better understanding of the present observations. This model starts with the theoretical rotational energy transfer cross sections of Zarur and Rabitz,[12] which were calculated using an effective potential formalism. State-to-state energy transfer rate constants are determined for a given translational temperature by integrating the energy dependence of the cross section over a Maxwell-Boltzmann velocity distribution. The rate constants are used in the master equations of kinetics, which are coupled to the fluid mechanical equations appropriate to a one-dimensional uniform flow under steady-state conditions (Ref. 8, Eq. 25). The unknowns in this set of first order differential equations are: $P_i(x)$, the population of state i; $T(x)$, the translational temperature; $v(x)$, the flow velocity; $p(x)$, the local pressure; $A(x)$, the cross sectional area of the flow; and $\rho(x)$, the number density. Here x is the distance along the flow from the orifice. Following Rabitz and Lam we have assumed the Ashkenas-Sherman[13] formula (with either two or three terms) for the Mach number at x greater than x*, and an exponential form at x less than x* (Ref. 8, Eqs. 37,38). The parameter x* is typically chosen to be equal to one nozzle diameter. The number density $\rho(x)$ can be calculated from the isentropic equation relating it to the Mach number,

$$\rho(x) = \rho_0 \left(1 + (1/2)(\gamma - 1)\, M(x)^2\right)^{1/(1-\gamma)} \qquad (3)$$

where ρ_o is the stagnation number density, M(x) is the Mach number, and $\gamma = C_p/C_v$. To facilitate a numerical solution, Eq. 25 of Ref. 8 was manipulated into the following set of differential equations,

$$\frac{dP_i}{dx} = \frac{\rho}{v} \sum_j \sum_\ell \sum_{m \geq \ell} \left(- P_i P_j k(ij\ell m;T) + P_\ell P_m k(\ell m ij;T) \right) G(ij\ell m) \quad (4a)$$

$$\frac{dT}{dx} = \frac{2}{3} T \left(\frac{1}{\rho} \frac{d\rho}{dx} - \frac{1}{kT} \sum_i \epsilon_i \frac{dP_i}{dx} \right) \quad (4b)$$

$$\frac{dv}{dx} = - \frac{1}{m_o v} \left(\frac{5}{2} k \frac{dT}{dx} + \sum_i \epsilon_i \frac{dP_i}{dx} \right) \quad (4c)$$

$$\frac{d\rho}{dx} = - \rho m_o v \frac{dv}{dx} \quad (4d)$$

$$\rho v A = \text{constant} \quad (4e)$$

where $G(ij\ell m)$ is a symmetry factor (defined in Ref. 8), ϵ_i is the rotational energy of state i, m_o is the mass of H_2, and $k(ij\ell m;T)$ is the rate constant for the process,

$$H_2(i) + H_2(j) \rightarrow H_2(\ell) + H_2(m) \quad (5)$$

The rate constants must be recalculated for the new T(x) at each step in the integration. We used a cubic least-squares fit to each of the cross sections, $\sigma(ij\ell m;E)$ vs. E in Table V of Ref. 12 (corrected as per Note 10 of Ref. 8), so that the necessary integrals over the velocity distribution could be evaluated analytically. It should be

noted that only the low kinetic energy region is of importance when calculating k(ijℓm;T) for T less than 300K. Hence the least-squares fit included only the values of the cross section with kinetic energies less than 0.3 eV. Eqs. (4) were integrated with a fourth-order Runge-Kutta routine for $-4 \leq (x/d) \leq +4$, for a range of initial values which included the starting conditions used in the present measurements. These calculations included the rotational levels of p-H_2 with J=0, 2, and 4.

Fig. 10 shows the rotational populations of p-H_2 measured with the 70 μm nozzle at 297K, together with the calculated curve. In Fig. 9 the calculated curve for the rotational energy as a function of $(Kn_0)^{-1}$ appears with the experimental points for p-H_2. The comparison between theory and experiment is somewhat clouded by the uncertainty in the assumed form of $\rho(x)$ in Eq. 3. The adjustable parameters at our disposal are γ, x*, and the number of terms in the Ashkenas-Sherman formula (either two or three). The heat capacity ratio appropriate to this problem is likely to lie somewhere between the monatomic ($\gamma = 1.67$) and the diatomic ($\gamma = 1.40$) values. The number density measurements of Godfried, et al.[6] for pd = 300 torr-mm suggest that the monatomic value is the correct one for n-H_2 at $x/d > 1$. It will be seen below that the rotational relaxation is essentially confined to the region where $x/d < 1.5$, so that the observation of a monatomic-like number density profile at larger x/d is not too surprising. The Ashkenas-Sherman formula gives a poor description of the Mach number at small x/d where all the relaxation takes place. Therefore the choice of x*, which is the point

where the exponential extrapolation to small x begins, is expected to have an appreciable effect on the results. Because of the importance of the small x/d region, it seems advisable to use the three term formula for M(x) (which is valid down to x/d = 1.0, according to Ref. 13) rather than the two-term formula which was adopted by Rabitz and Lam. The calculated curves in Figs. 9 and 10 were generated by using $\gamma = 1.40$ and $x^*/d = 0.8$ with the three-term formula for M(x). The rotational energy curve in Fig. 9 shifts downward for larger values of γ or x^*, yielding poorer agreement with experiment. The curve shifts upward if the two-term formula is used, yielding somewhat better agreement with experiment. The model of Rabitz and Lam is thus confirmed to be a fairly realistic one, but the remaining uncertainty about $\rho(x)$ seems to preclude a more definitive test of the correctness of the rotational energy transfer cross sections.

A very valuable aspect of this model is the detailed picture that it gives of the dynamics of the free jet expansion. As an example of this we show in Fig. 11 the populations $P_0(x)$, $P_2(x)$, and $P_4(x)$, and the values of $\rho(x)$, T(x), v(x), $\sqrt{A(x)}$, and p(x) calculated for a stagnation pressure of 1600 torr. It can be seen that the rotational populations have approached their asymptotic values for $x/d \simeq 1.5$, at which point the temperature is about 65K and the Mach number is about 3. The temperature actually continues to cool until much further downstream, and the Mach number reaches a terminal value estimated to be between 10 and 20 (cf. Ref. 4). Rotational relaxation ceases for x/d greater than 1.5 primarily because the energy transfer rate

constants have dropped by several orders of magnitude from their room temperature values (see Ref. 8, Fig. 1). In this model the temperature profile, T(x), is nearly independent of the stagnation pressure. Thus the effect of increasing the pressure is simply to increase the number of collisions that occur before the temperature is too low for R-T energy transfer. This point is reached at $x/d \simeq 1.5$ for all stagnation pressures.

We have shown that the theoretical approach of Rabitz and Lam can give a rather good account of the rotational relaxation in a free jet of $p\text{-}H_2$. It would be of interest to apply this method to HD if the necessary cross sections become available, to see how well the model predicts the much more facile relaxation that we have observed for this system.

Finally we note that the state-specific detection of molecular hydrogen has recently been achieved by Marinero, Rettner, and Zare[14] using a three-photon ionization technique. This method could in principle be extended to samples with number densities as low as 10^8 cm^{-3} and could provide a very sensitive means for studying the rotational relaxation in a supersonic expansion of hydrogen.

ACKNOWLEDGMENT

This work is supported by the Director, Office of Energy Research, Office of Basic Energy Sciences, Chemical Sciences Division of the U.S. Department of Energy under Contract No. DE-AC03-76SF00098.

REFERENCES

1. D. Bassi, A. Boschetti, S. Marchetti, G. Scoles, and M. Zen, J. Chem. Phys., 74, 2221 (1981); and references cited therein.
2. J. E. Pollard, D. J. Trevor, J. E. Reutt, Y. T. Lee, and D. A. Shirley, J. Chem. Phys. (in press).
3. R. J. Gallagher and J. B. Fenn, J. Chem. Phys., 60, 3487 (1974); and 60, 3492 (1974).
4. U. Buck, F. Huisken, J. Schleusener, and J. Schaefer, J. Chem. Phys., 74, 535 (1981); and J. Andres, U. Buck, F. Huisken, J. Schleusener, and F. Torello, J. Chem. Phys., 73, 5620 (1980).
5. J. Verberne, I. Ozier, L. Zandee, and J. Reuss, Mol. Phys., 35, 1649 (1978).
6. H. P. Godfried, I. F. Silvera, and J. Van Straaten, 12th International Symposium on Rarefied Gas Dynamics (Charlottesville, 1980) part 2, p. 772.
7. P. Huber-Wälchli and J. W. Nibeler, J. Chem. Phys., 76, 273 (1982).
8. H. Rabitz and S.-H. Lam, J. Chem. Phys., 63, 3532 (1975).
9. J. E. Pollard, D. J. Trevor, Y. T. Lee, and D. A. Shirley, Rev. Sci. Instrum., 52, 1837 (1981).
10. Y. Itikawa, Chem. Phys., 30, 109 (1978).
11. Y. Morioka, S. Hara, and M. Nakamura, Phys. Rev. A, 22, 177 (1980).
12. G. Zarur and H. Rabitz, J. Chem. Phys., 60, 2057 (1974).

13. H. Ashkenas and F. S. Sherman, 4th International Symposium on Rarefied Gas Dynamics (Toronto, 1964) vol. 2, p. 84.

14. E. E. Marinero, C. T. Rettner, and R. N. Zare, Phys. Rev. Lett., 48, 1323 (1982).

Table I. Rotational energies (in cm^{-1}) and degeneracies for the v=0 level in the ground electronic state of n-H_2, HD, and n-D_2.

	n-H_2		HD		n-D_2	
J	E_J	g_J	E_J	g_J	E_J	g_J
0	0.	1	0.	1	0.	6
1	118.49	9	89.24	3	59.77	9
2	354.37	5	267.09	5	179.04	30
3	705.51	21	532.36	7	357.26	21
4	1168.76	9	883.26	9	593.63	54
5	1740.09	33	1317.48	11	887.05	33
6	2414.74	13	1832.28	13	1236.18	78

Energies are derived from the rotational constants of K. P. Huber and G. Herzberg, Constants of Diatomic Molecules, Van Nostrand Reinhold, New York (1979).

Table II. Rotational population distributions in some high Mach number expansions of n-H_2 and n-D_2.

	p(torr)	d(μm)	T(K)	J=0	J=1	J=2	J=3	J=4	J=5	J=6
H_2										
	1830	70	297	19.5	70.8	6.8	2.8	0.1		
	2350	70	480	14.2	59.0	12.3	12.8	0.8	0.9	
	11100	40	297	21.2	75.1	2.9	0.8			
	19000	40	492	19.4	69.6	7.3	3.7			
	32000	40	696	23.0	63.0	8.7	5.3			
D_2										
	1830	70	297	33.2	28.5	31.0	4.5	2.5	0.3	
	1420	70	475	18.6	19.9	34.6	12.0	11.2	1.9	1.8
	8600	40	297	46.2	31.8	19.8	1.3	0.9		
	24000	40	505	41.5	31.7	23.7	1.8	1.2	0.1	
	40000	40	694	34.3	31.8	28.2	3.6	2.0	0.1	

FIGURE CAPTIONS

Fig. 1. The v'=5 transition from n-H_2 expanded through a 40μm nozzle at 696K for several stagnation pressures. The transitions are labeled with the Q branch rotational quantum numbers.

Fig. 2. Rotational populations of n-H_2 and n-D_2 expanded through a 70μm nozzle at 297K.

Fig. 3. Plot of $\ln(n_J/g_J)$ versus E_J for n-H_2 and n-D_2 expanded through a 70μm nozzle at 1830 torr.

Fig. 4. Two-level temperatures (relative to J=0) for n-H_2 and n-D_2 expanded through a 70μm nozzle at 1830 torr.

Fig. 5. Fraction of retained rotational energy vs. inverse Knudsen number for n-H_2 with the nozzle diameters and stagnation temperatures indicated. E_T is the initial energy, and E_0 is the energy at zero K for a 3:1 ortho-para ratio (88.87 cm^{-1}).

Fig. 6. Fraction of retained rotational energy vs. inverse Knudsen number for n-D_2 with the nozzle diameters and stagnation temperatures indicated. E_T is the initial energy, and E_0 is the energy at zero K for a 2:1 ortho-para ratio (19.92 cm^{-1}).

Fig. 7. Rotational populations of HD expanded through a 70μm nozzle at 297K.

Fig. 8. Plot of $\ln(n_J/g_J)$ versus E_J for HD expanded through a 70μm nozzle at several stagnation pressures. The lines are

weighted least-squares fits to the data. They correspond to rotational temperatures of 273K, 210K, 145K, and 99K, for 25, 100, 400, and 1830 torr, respectively.

Fig. 9. Fraction of retained rotational energy vs. inverse Knudsen number for p-H_2 and HD with a 70μm nozzle at 297K. The curve is the result of the calculation which is explained in the text.

Fig. 10. Rotational populations for the J=0, 2, and 4 levels of p-H_2 expanded through a 70μm nozzle at 297K. The curves are the results of the calculation which is explained in the text.

Fig. 11. Model calculation of the p-H_2 expansion with a 70μm nozzle at 297K and 1600 torr stagnation pressure. x/d is the distance in nozzle diameters along the centerline from the orifice. The upper graph shows the populations of the J=0, 2, and 4 rotational states. The lower graph shows the number density ρ, the translational temperature T, the flow velocity v, the square-root of the cross sectional area $\sqrt{A}$, and the local pressure p, all normalized to fit on the same scale. This calculation uses the three-term Ashkenas-Sherman formula for the Mach number and assumes $\gamma = 1.40$ and $x^*/d = 0.8$.

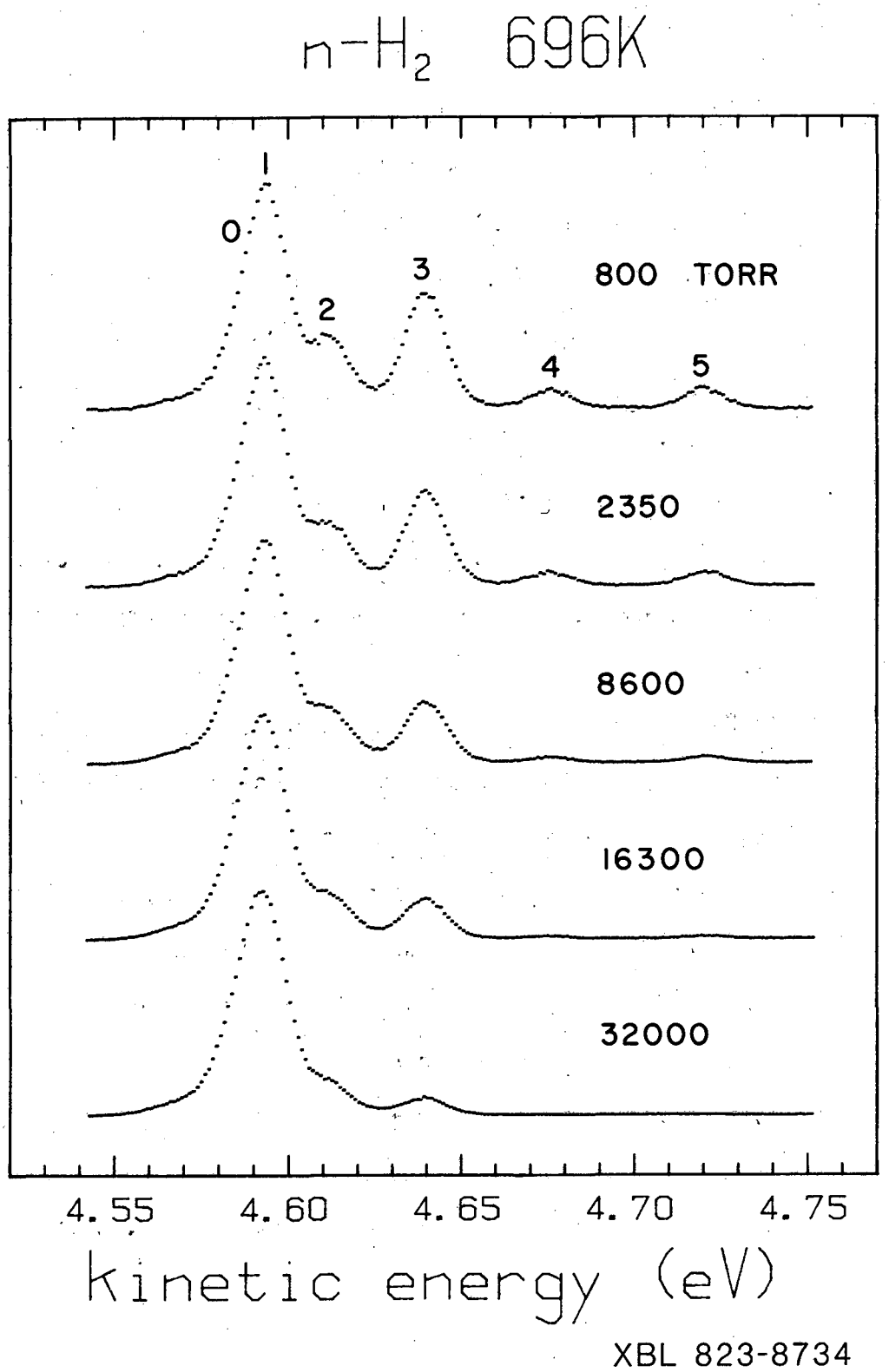
n-H2 696K
0
1
2
3
4
5
800 TORR
2350
8600
16300
32000
4.55
4.60
4.65
4.70
4.75
kinetic energy (eV)
XBL 823-8734

Figure 1

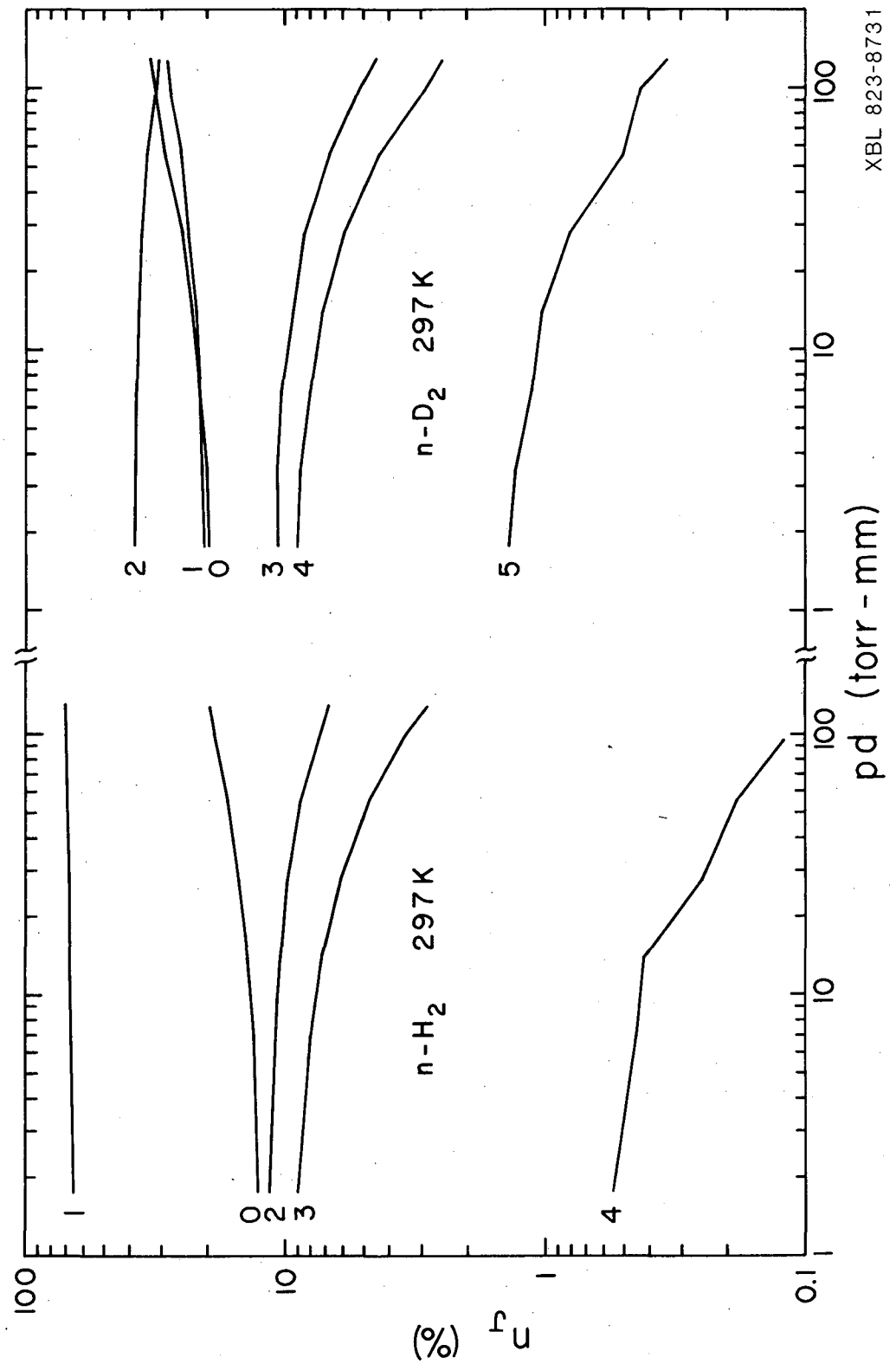
100
10
1
0.1
η_J (%)
1
0
2
3
4
n-H_2 297 K
2
1
0
3
4
5
n-D_2 297 K
1
10
100
pd (torr - mm)
XBL 823-8731

Figure 2

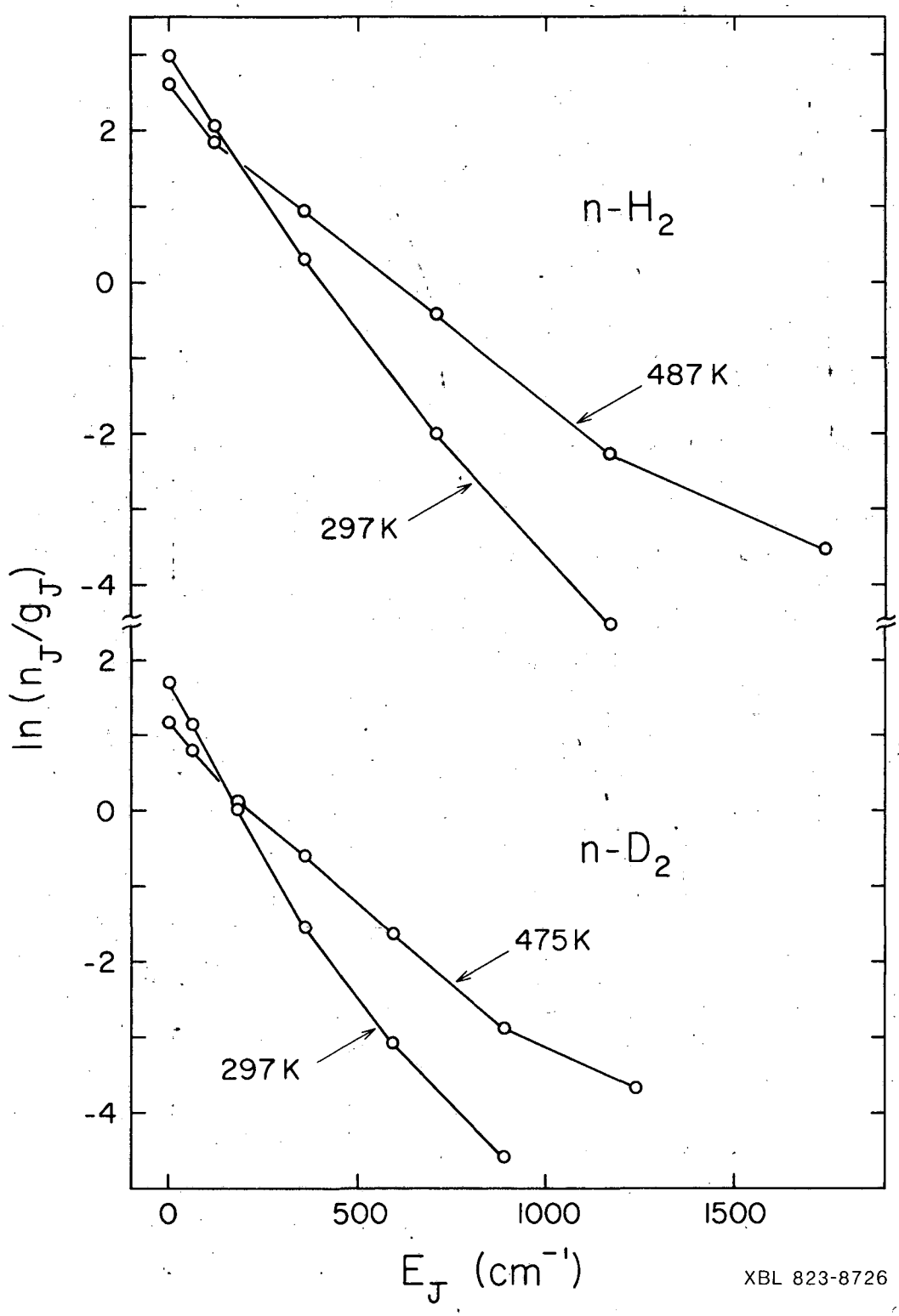
n-H2
487 K
297 K
n-D2
475 K
297 K
ln (nJ/gJ)
EJ (cm-1)
2
0
-2
-4
500
1000
1500
XBL 823-8726

Figure 3

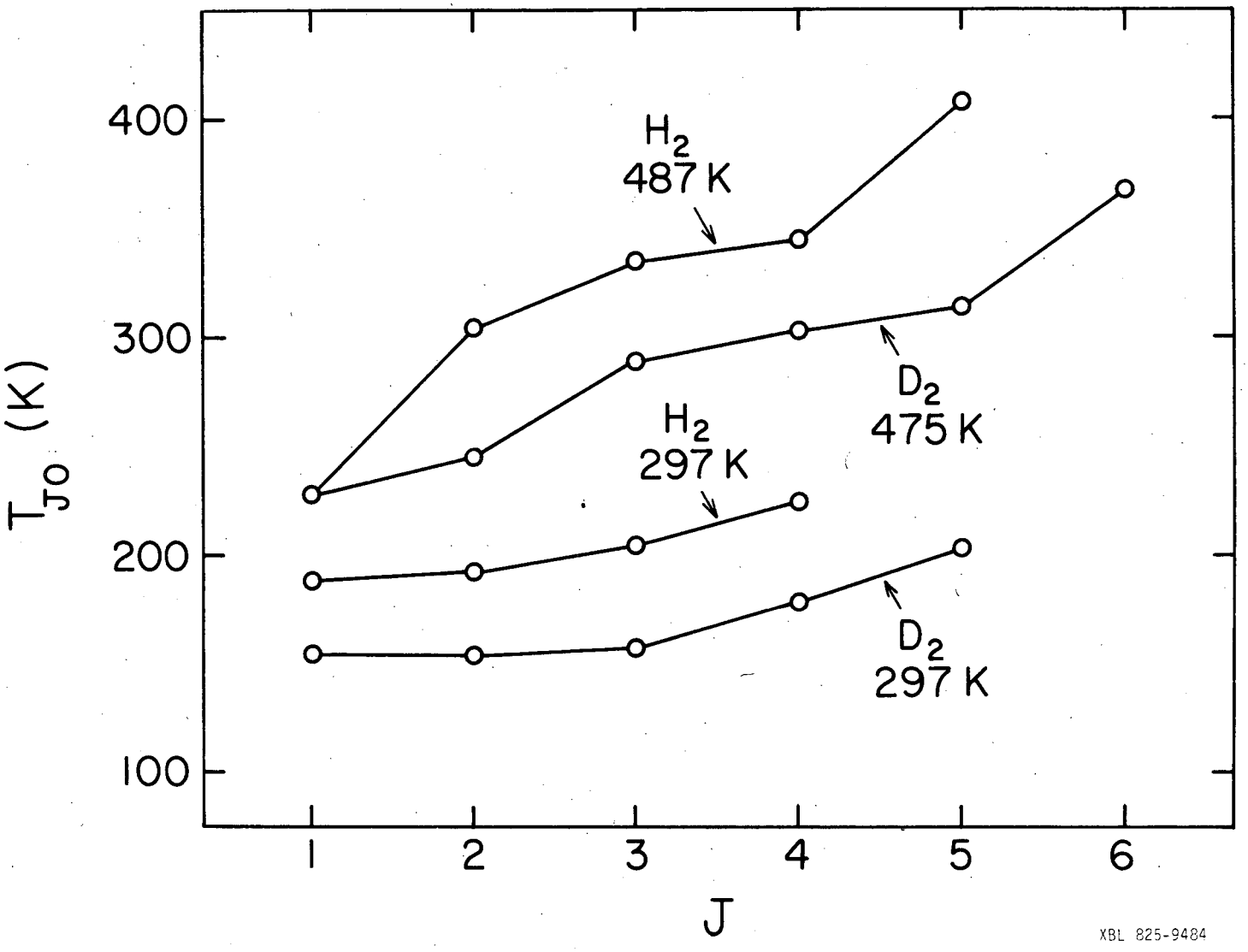
400
300
200
100
T_{J0} (K)
1
2
3
4
5
6
J
H_2
487 K
D_2
475 K
H_2
297 K
D_2
297 K
XBL 825-9484

Figure 4

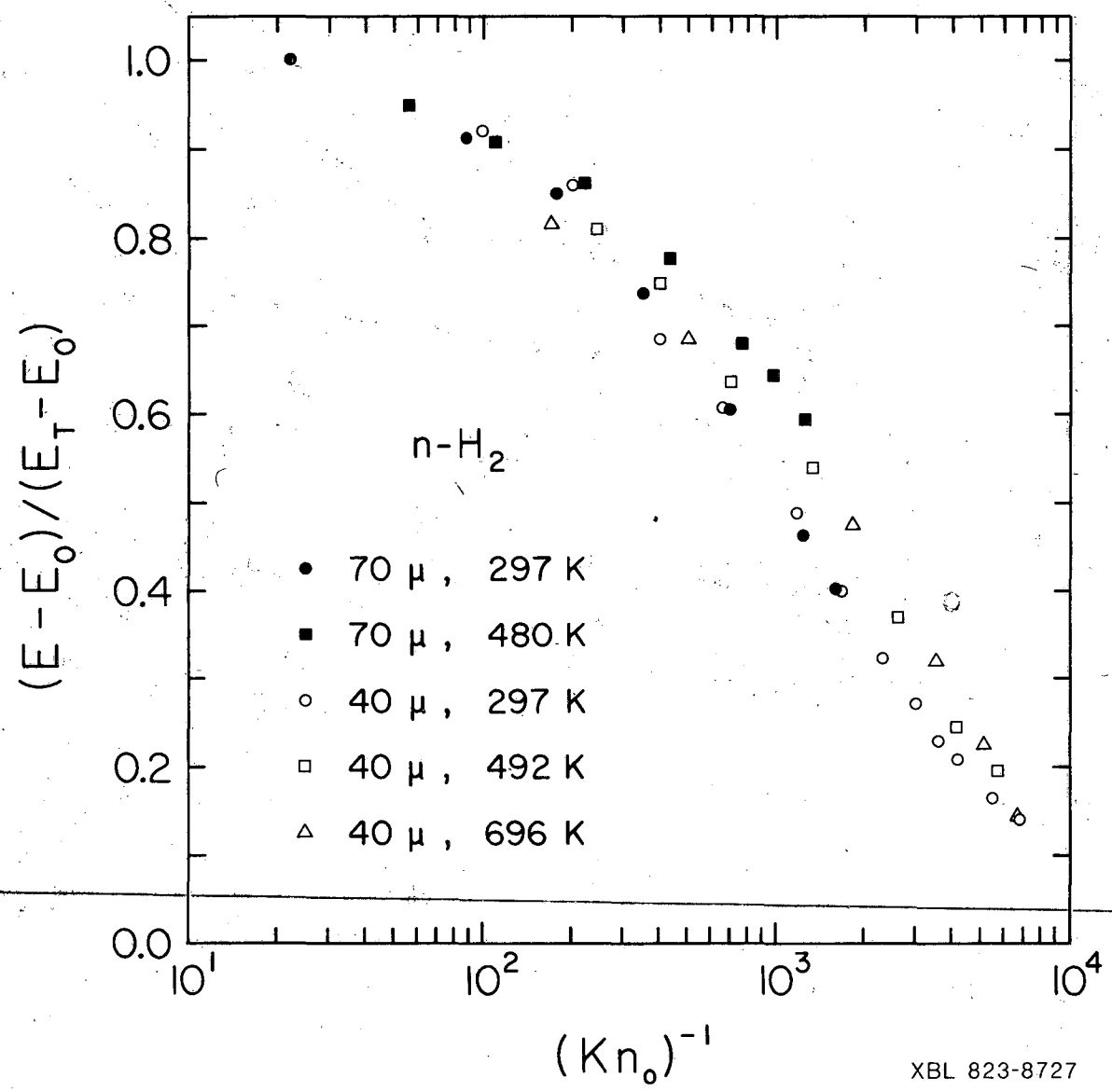
1.0
0.8
0.6
0.4
0.2
0.0
$(E-E_0)/(E_T-E_0)$
$n\text{-}H_2$
70 μ , 297 K
70 μ , 480 K
40 μ , 297 K
40 μ , 492 K
40 μ , 696 K
10^1
10^2
10^3
10^4
$(Kn_0)^{-1}$
XBL 823-8727

Figure 5

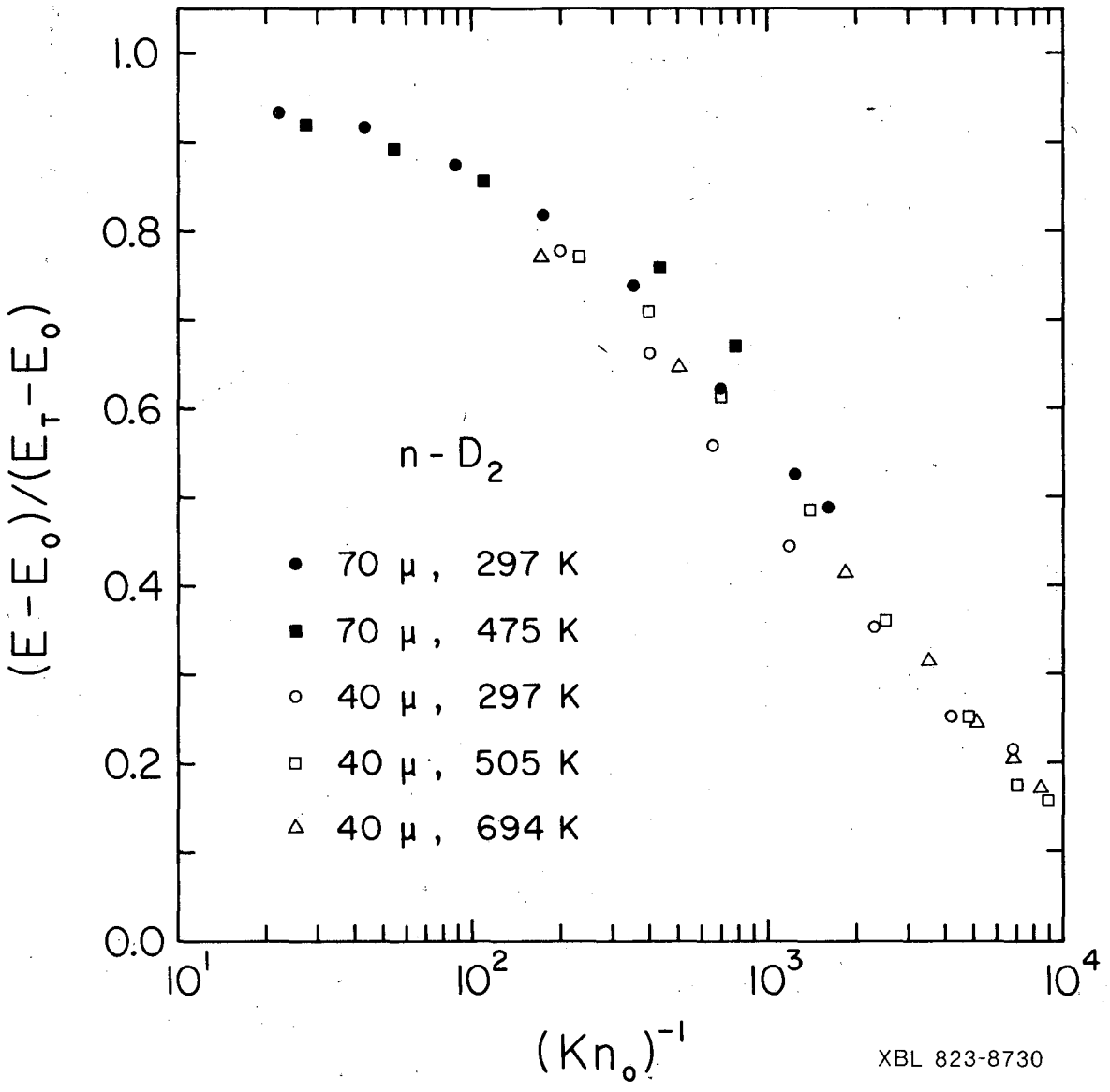
1.0
0.8
0.6
0.4
0.2
0.0
$(E-E_o)/(E_T-E_o)$
n - D_2
70 μ, 297 K
70 μ, 475 K
40 μ, 297 K
40 μ, 505 K
40 μ, 694 K
10^1
10^2
10^3
10^4
$(Kn_o)^{-1}$
XBL 823-8730

Figure 6

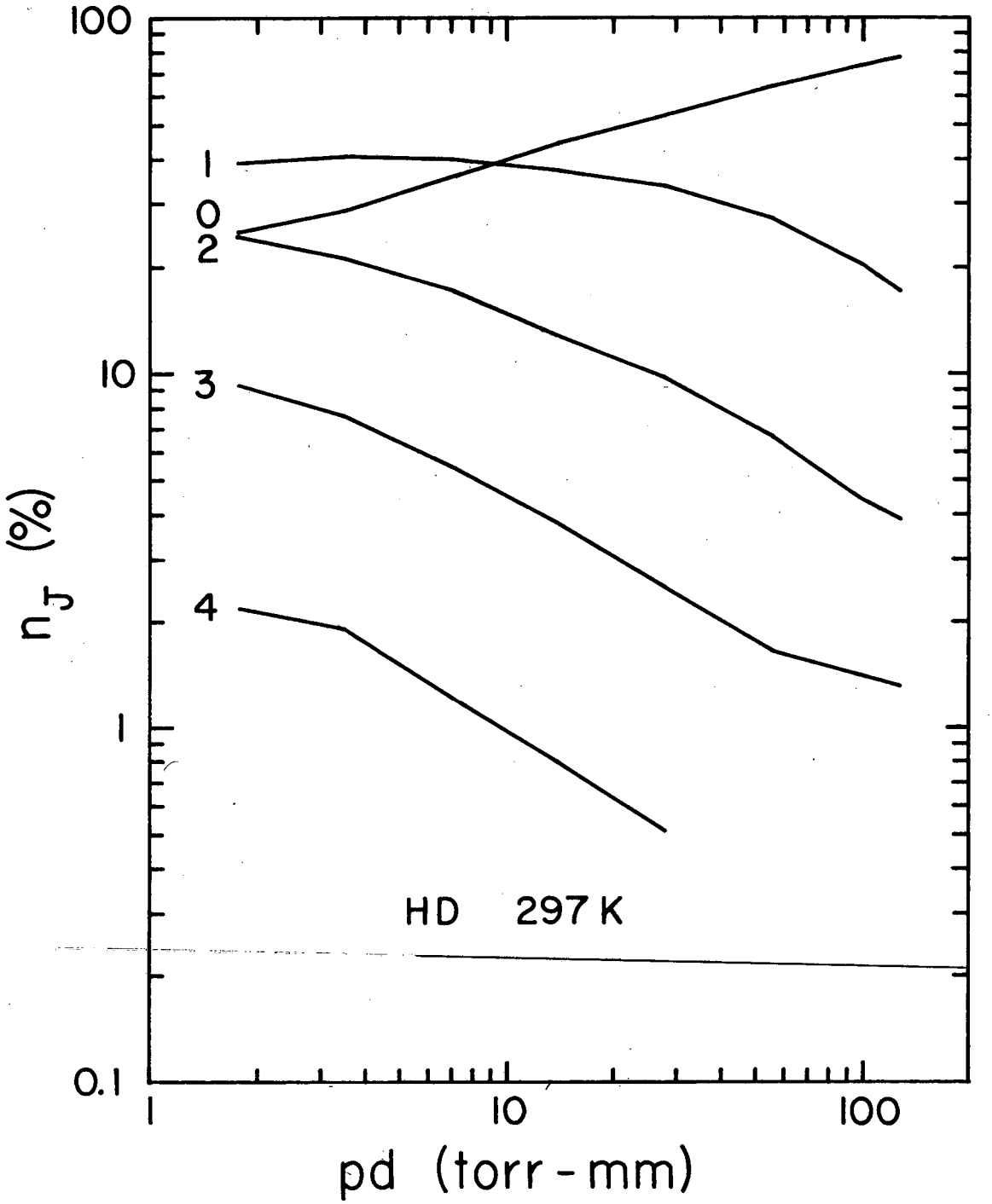

Figure 7

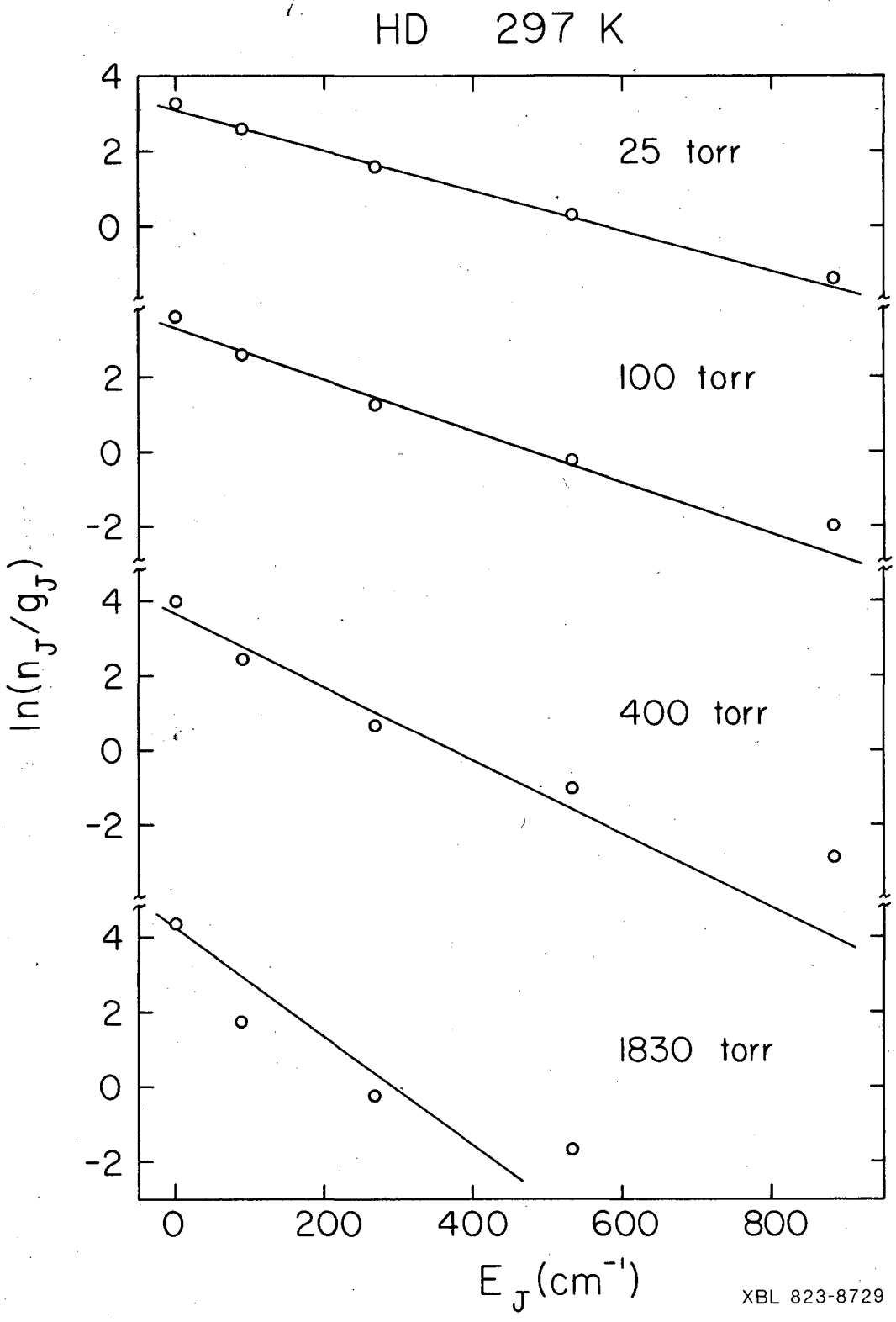
HD 297 K
25 torr
100 torr
400 torr
1830 torr
$\ln(n_J/g_J)$
$E_J(cm^{-1})$
0
200
400
600
800
4
2
0
-2
XBL 823-8729

Figure 8

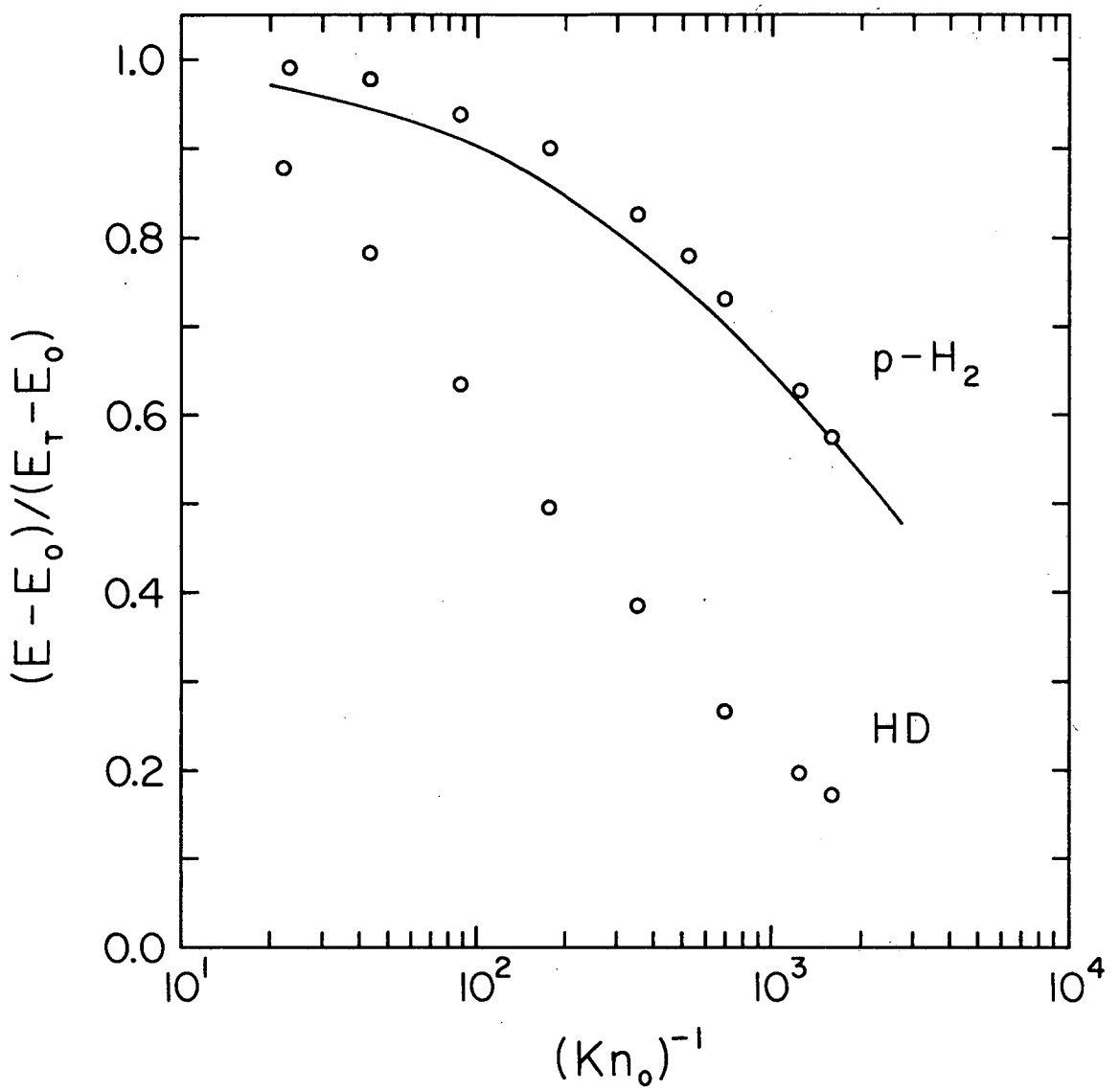

XBL 824-9113

Figure 9

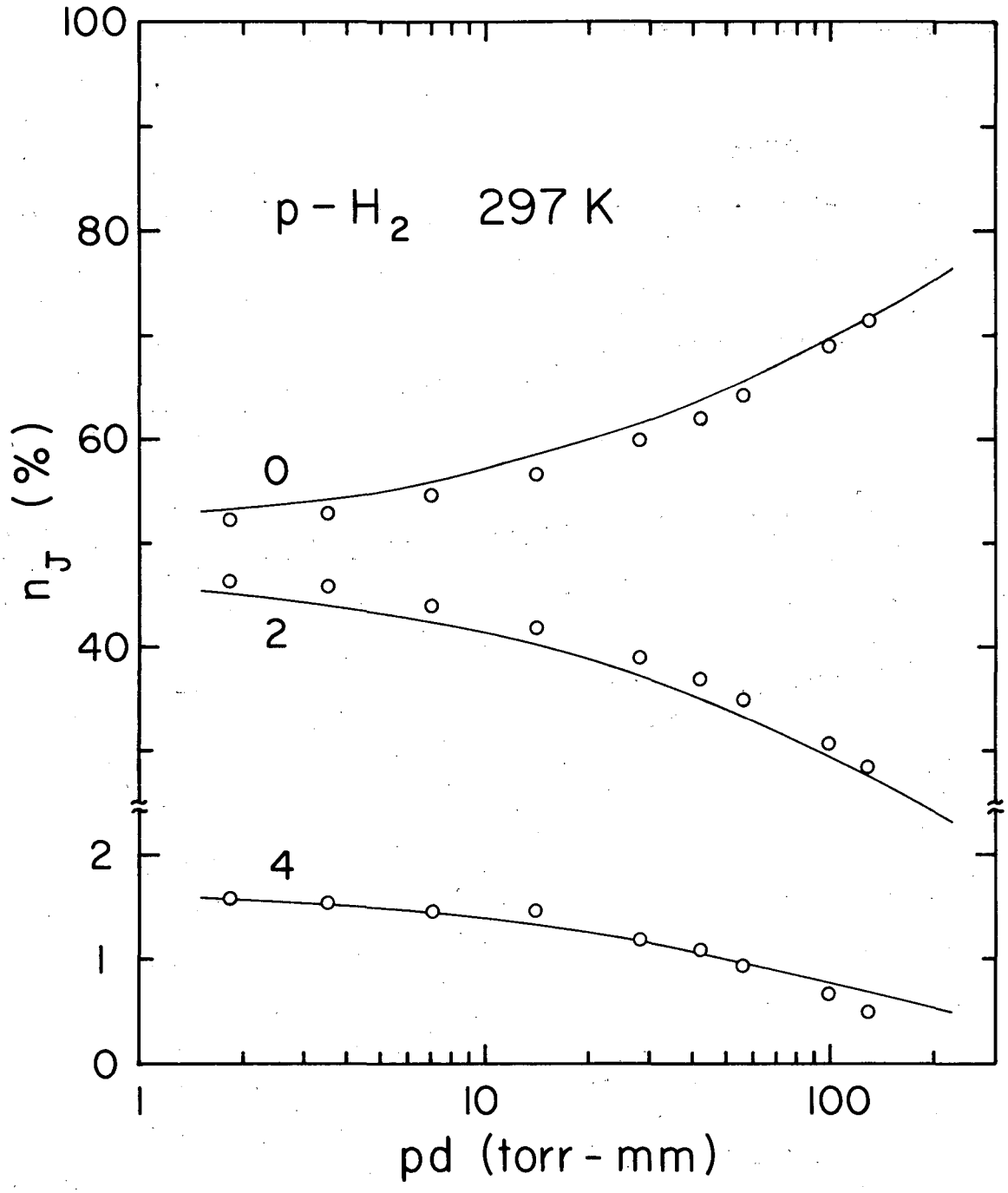

XBL 824-9114

Figure 10

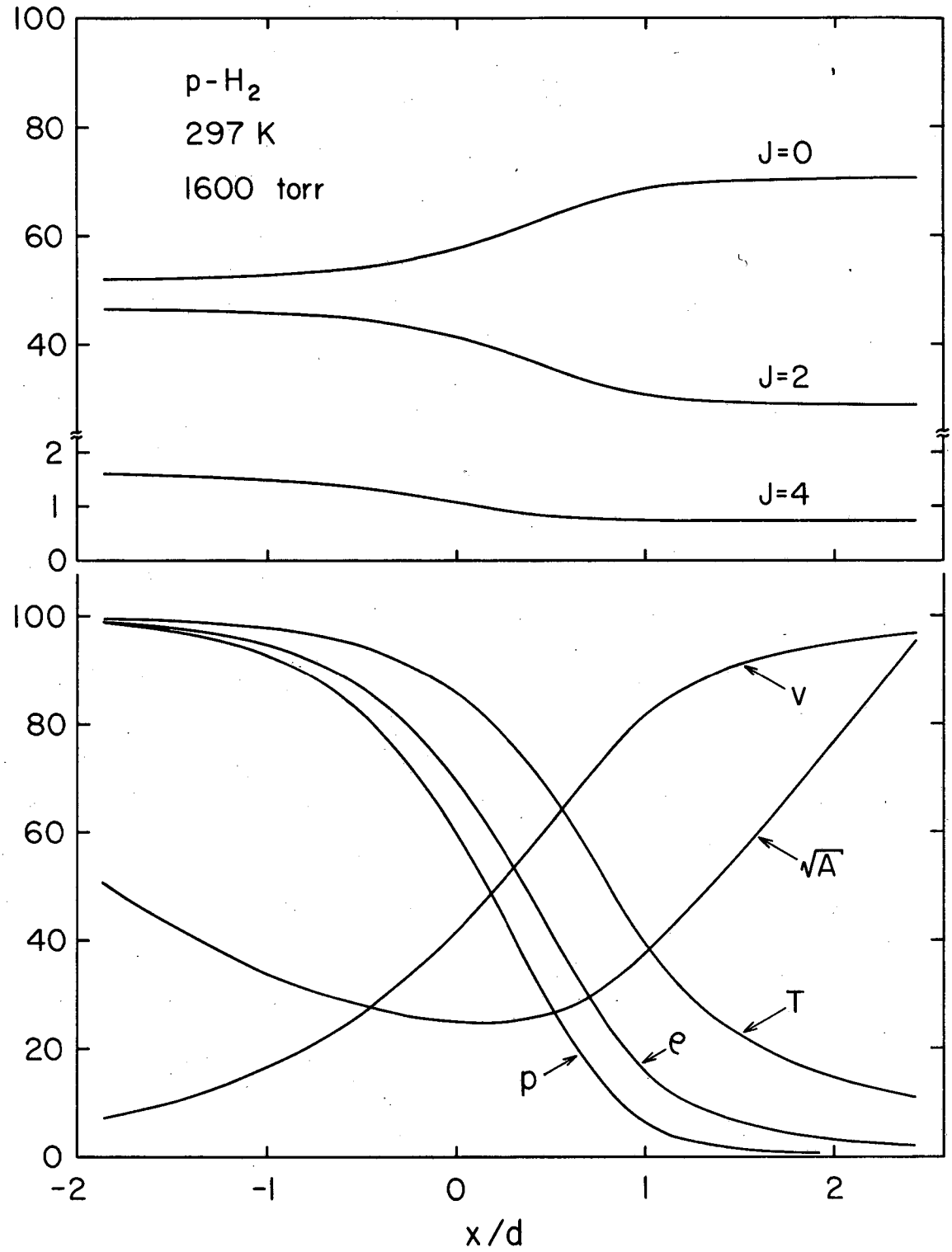

XBL 824-9112

Figure 11

TECHNICAL INFORMATION DEPARTMENT
LAWRENCE BERKELEY LABORATORY
UNIVERSITY OF CALIFORNIA
BERKELEY, CALIFORNIA 94720